

Lifting Some Secrets About Contrast Pyramids

Institute of Visual Computing and Human-Centered Technology, Virtual and Augmented Reality, E193-03, Technische Universität Wien, 1040 Vienna, Austria krw@prip.tuwien.ac.at

Abstract. Contrast pyramids have shown excellent reconstructions for several images with only a few number of high contrasts. The contrast histogram of the image shows the distribution of contrasts and allows to select a bound that limits the mean reconstruction error. A total order of the vertices enables a both the ordering of the edges with the same contrast and, together with max-link strategy, generates efficiently the contraction kernels of the pyramid. A spiral total order pushes the surviving vertices geometrically towards the center of the image.

Keywords: Spiral total order \cdot Image Pyramids \cdot Error Bound of Reconstruction

1 Introduction

There have been several attempts to build hierarchies to cope with the huge amount of data. Table 1 outlines the main categories, their signal processing categories and their underlying data structures. When building a graph pyramid one basic question relates to the space and time requirements of the related processes:

(1) how many edges are contracted after reaching a certain level? and (2) How many edges can be removed? In order to answer the two questions let us recall the basic properties of graph pyramids (see also the 3×4 example in Fig. 1). The base graph $G_0 = (V_0, E_0)$ has as many vertices as there are pixels in the $m \times n$ 2D image, then the base graph contains |V0| = mn vertices. Edges E_0 connect vertices of neighboring pixels. Assuming 4-neighborhood (graphs of 8-neighborhood would not be planar) in the images we have $|E_0| = 2mn - m - n$ edges.

We first recall the basic concepts of building a pyramid of graphs that preserves high image

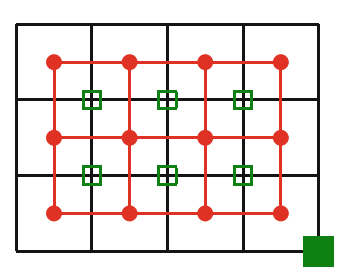


Fig. 1. 3×4 image, graph $G_0(\text{red})$ and dual face graph $\overline{G_0}$ (green) with background \blacksquare (Color figure online)

[©] The Author(s), under exclusive license to Springer Nature Switzerland AG 2025 L. Brun et al. (Eds.): GbRPR 2025, LNCS 15727, pp. 235–245, 2025. https://doi.org/10.1007/978-3-031-94139-9_22

Hierarchy	signal	data	more details
Gaussian pyramids	lowpass	rigid array	[8]
Laplacian pyramids	bandpass	rigid array	[8]
Wavelets	bandpass	rigid array	[14]
Graph neur.netw.	message passing	rigid graph	[5]
Graph pyramid	highpass	multigraph	[13]

Table 1. Hierarchies, their signal and data characteristics

contrasts (Sect. 2). Then Sect. 3 computes the contrast histogram directly from the original image as a pre-processing step. A total order on the graph's vertices in Sect. 4 defines the order of edges that have the same contrast. The extremely efficient max-link strategy generates from the spiral total order a spanning tree that can be directly used for constructing the contrast pyramid. Finally the contrast histogram of a given image allows to predict an upper bound for the mean error of reconstruction.

2 Recall on the Irregular Contrast Pyramid

2.1 Edge Contractions and Removals

The only operations to generate higher pyramid levels are **edge contractions** and **edge removals** [6]. The operation of contracting an edge deletes the edge and one of its end points (the other "**survives**") while the removal of an edge deletes the edge and merges its adjacent (dual) faces. A set of edges that are contracted with the same surviving vertex are called **contraction kernels** (**CK**) and all the edges to remove are called **removal kernels** (**RK**). The result of contracting graph G by a contraction kernel CK is denoted G/CK, the result of removing a removal kernel RK: $G \setminus RK$.

To properly preserve inclusion relationships and topology not all parallel edges and self-loops resulting from edge contractions can be removed. Contracting a **double edge** $e_1 = (v, w) \in E$ with $e_2 = (v, w) \in E$ creates a self-loop $e_2 = (v, v)$ if $v \in V$ survives. Contracting one of multiple parallel edges (v, w) creates one less self-loops as there were multiple edges connecting the same pair of vertices. Self-loops $(v, v) \in E$ cannot be contracted since the two end points are already the same vertex. They can only be removed.

The concept of **equivalent contraction kernels (ECK)** [12] allows to combine multiple contraction kernels resulting in the same simpler graph than several successive contractions. Similar to the concept of ECK the removed edges are combined in the **equivalent removal kernel, ERK**. The **receptive field** $RF(v_t) \subset V_0$ of a higher level vertex $v_t \in V_t, t > 0$, can be derived directly from the base by the ECK of v_t that is a tree spanning the receptive field of v_t . The receptive fields of a graph $G_t = (V_t, E_t)$ at a level t > 0 partition the base vertices, $V_0 = \bigcup_{v \in V} RF(v_t)$ the receptive fields are the connected components

of the spanning forest of the base graph G_0 . Every ECK contracts $|RF(v_t)| - 1$ edges to collapse all the covered vertices of V_0 into a single surviving vertex v_t . All together $\sum_{v_t \in V_t} (|RF(v_t)| - 1) = |V_0| - |V_t|$ edges need to be contracted to reach G_t from G_0 .

2.2 Only Contractions Without Removals

The top graph $G_t(V_t, E_t)$ of the pyramid can be a single vertex, e.g. $|V_t| = 1$. $|V_0| - 1$ edges are contracted and the remaining edges E_r are not removed. Since there is only one vertex left, all the remaining edges E_t are self-loops. Due to the inheritance of contrast, the contrast attribute of the self-loops corresponds to the highest contrast in the equivalent cycle in G_0 . In terms of pixels this means that $|E_c| = nm - 1$ and $|E_t| = (m-1)(n-1)$.

The top level consists of a single vertex $|V_t| = 1$ and self-loops E_t in different topological constellations (examples in Figs. 4(b), (c), 5(b), (c)). The number of top edges $|E_t| = (m-1)(n-1)$ corresponds exactly to the number of non-background faces of the dual graph (the 2×3 green vertices in Fig. 1).

3 Contrast Histogram

The structure of the pyramids constructed by Cerman and Batavia et al. [3,10] are determined by following main properties: (1) low contrast edges contract before higher contrast edges; (2) the spatial arrangement of critical points with high contrast is preserved; and (3) independence criteria for parallel application. The local contrast c(v, w) of an edge $(v, w) \in E$ compares the grey values g(v), g(w), with $v, w \in V$, $0 \le g(v), g(w) \le G_{max}^{-1}$, of two 4-adjacent pixels (Fig. 2).



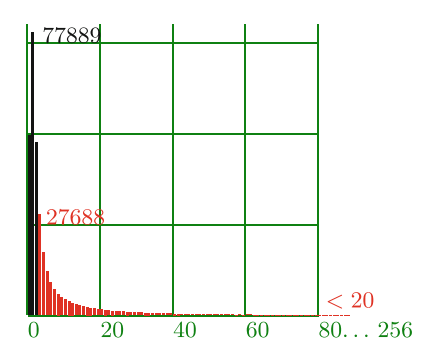


Fig. 2. 481×321 image of pheasant with contrast histogram. The red bars in the contrast histogram mark the surviving edges. (Color figure online)

 $[\]overline{G_{max}}$ is the largest grey value, in most cases 255.

Definition 1 (Contrast Histogram). Let $(v, w) \in E$ be two neighboring vertices of the image. The distribution of local contrasts c(v, w) of a digital image counts the frequency of the different contrasts $0 \le c_i \le G_{max}$:

$$h_0(c_j) = |\{(v, w) \in E | c(v, w) = c_j\}| \tag{1}$$

3.1 Pre-selection of Parameters

The top level of the pyramid is reached after contracting edges with $c(v, w) < c_t, v \neq w$, and contains the representatives of the $|E_t|$ surviving edges from the base level E_0 with largest contrasts. In the SCIS concept of Cerman etal [10] edges with lowest contrast are contracted first, then redundant edges are removed before iterating contraction and removal with higher contrasts until reaching the selected top level.

Using h_0 , the edges can be brought into the canonical ordering [16] **before** actually starting the contraction process. The use of h_0 avoids to sort of the edges to determine the next block of edges with lowest contrast. However the order of the edges with the same contrast is not determined by the data. For those edges we pre-compute a total order of vertices (see below).

Edges that connect vertices of the same subtree of the ECK collapse into a self-loop after G/ECK. If their contrast is below c_t they are considered **redundant**. These edges can be removed before the contractions start. Reverse operations (for reconstruction) use the reverse canonical order. The original graph is completely reconstructed, only the attributes like the pixel value or the edge contrast may vary.

In the contrast histogram we know beforehand how many edges have contrast 0: $h_0(0)$, contrast 1: $h_0(1)$ etc. We also know that the redundant parallel edges and self-loops created by the contractions of edges with contrast $h_0(k)$ are removed after contraction. Notice further that removal of an edge does not change vertices and, hence, no vertex attributes are lost by removing edges. Consequently one could bring the edges of the image into the canonical order from the contrast histogram before actually starting the pyramid construction.

4 A Total Order of Vertices in the Base Graph

We know that the ECKs of a high level of the pyramid form spanning forests of the receptive fields of the roots [12].

Definition 2 (Strict Total Vertex Order). Given a plane graph G(V, E) we define the rank of a vertex as a function $TO: V \mapsto [1, |V|]$ with binary relations TO(v) satisfying the following properties: irreflexive, asymmetric, transitive, and connected.

The (strict) total order of the vertices determine unique contraction kernels and, in addition, enable a large number of independent contraction kernels that can be contracted simultaneously with low parallel complexity.

Definition 3 (Independence). Two contraction kernels CK_a and CK_b are independent if their intersection $CK_a \cap CK_b = \emptyset$ does not contain any common vertex. Furthermore, in combinatorial maps [7] two edges are independent if they are not adjacent in the circular order around the same vertex.

4.1 Deriving Spanning Trees and Spanning Forests

 $ECK \subset E_0$ are spanning forests of the base graph.

Definition 4. Let G(V, E) denote the plane graph and $TO(v) : V \mapsto [1, |V|]$ be the rank of a vertex in the TO. The local neighborhood $\Gamma : V \mapsto V$ of a vertex $v \in V$ is defined by all vertices that are related by an edge in E:

$$\Gamma(v) = \{ w \in V | (v, w) \in E \text{ or } (w, v) \in E \}.$$

With max-link(TO), every vertex $w \in V \setminus R_{max}$ chooses the vertex $v \in \Gamma(w)$ that has the highest rank in the TO among the neighbors of v. (v, w) is then an edge of the ECK, T_{max} :

$$T_{max} = \{(v, w) \in E | w \in V \setminus R_{max}, \ TO(w) = \max_{v \in \Gamma(w)} \ TO(v) \}.$$
 (2)

The roots $R_{max} \subset V$ of each tree of the spanning forest $T_{max} \subset E$ are the local maxima of TO.

Proposition 1. The max-link algorithm (2) can be applied in parallel to all vertices of the graph. The parallel complexity depends only on the degree of the vertices and NOT on the number of vertices.

4.2 Column Major Order

A common total order follows the linear arrangement of pixels in a computer, called column major order (Fig. 3, [1]). The ECK contracts all the edges following the max-link strategy. Figure 4(a) shows both the ECK (in red) and the equivalent removal kernel (in green) that is not removed in this case (according

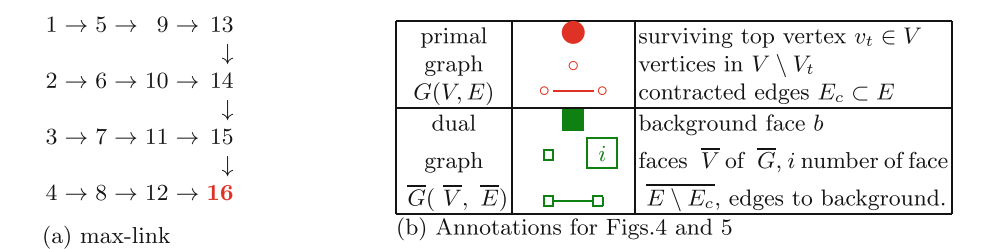


Fig. 3. Max-link of column major order, and annotations.

to Sect. 3.1). The background face b is added to the \overline{ERK} . We observe the general relation [4] between the spanning tree ECK of G(V, E) and the spanning tree \overline{ERK} of the dual face graph \overline{G} including the background face b:

$$\overline{ERK}(\overline{G}) = \overline{E \setminus ECK(G)} \tag{3}$$

Figure 4(b) shows the contracted graph G/ECK in red after contracting the maximal contraction kernel ECK without removing any parallel edges and self-loops. The nine surviving self-loops each surround one of the green dual faces and all self-loops connect to the root.

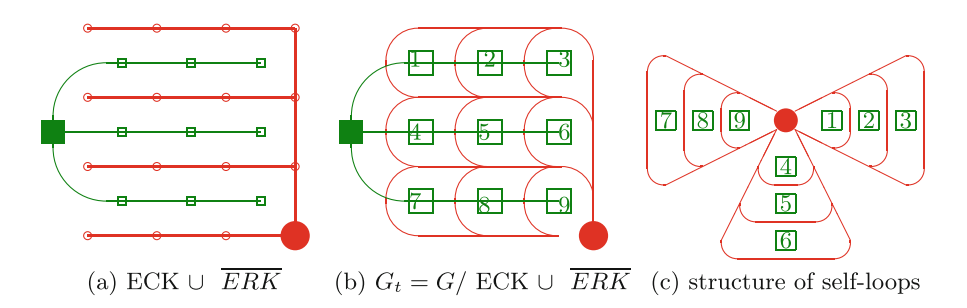


Fig. 4. 4 × 4 maximal contractions of column major TO (Color figure online)

To establish the correspondence between Fig. 4(b) and (c) the 9 faces have been numbered. Figure 4(c) shows the isomorphic unfolded graph and the structure of the self-loops of G/ECK. The three branches of the ERK, (1, 2, 3), (4, 5, 6), (7, 8, 9) correspond to the inclusions of self-loops along these branches.

4.3 Spiral Total Order

A second example, **spiral** in Fig. 5, shows an ECK_{spiral} that starts in the left lower corner of the image, and follows the pixels along a spiral curve in clockwise order. This path is Hamiltonian² and visits all vertices once.

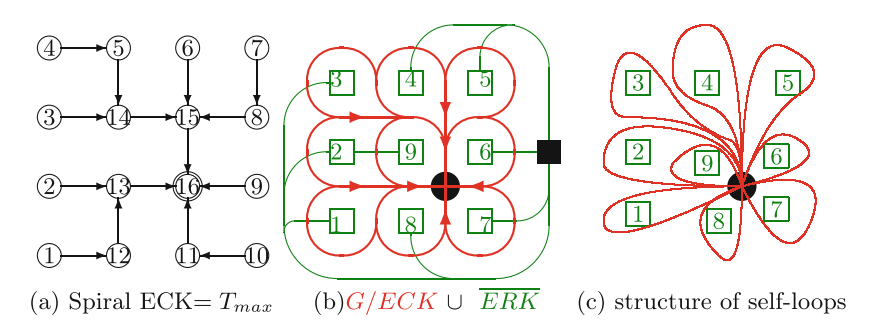


Fig. 5. 4×4 ECK of max-link of spiral.

 $^{^2}$ A Hamiltonian path is a path visiting every vertex of the graph exactly once.

ь

In Fig. 5(a) the TO of the spiral is transformed into another ECK= T_{max} by max-link. The result of the contractions G/ECK is the graph ($\{\bullet\}, E_t$) (Fig. 5(b)) with TO(\bullet) = 16 and 8 self-loops E_t directly attached to the root \bullet . Only the self-loop around $\boxed{2}$ includes self-loop $\boxed{9}$ in Fig. 5(c).

4.4 Properties of the Spanning Forests T

Figure 6 shows a rectangular 5×7 example and its max-link ECK (b).

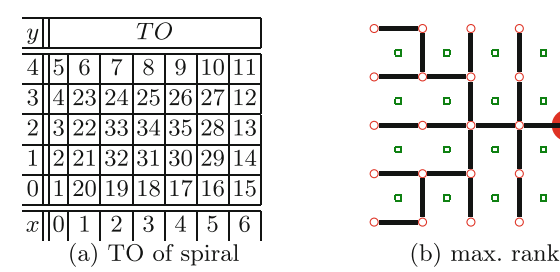


Fig. 6. Spiral: total order(TO) of the vertices

Proposition 2. Let TO denote the strict total order of vertices of graph G(V, E).

- In general the max-link algorithm (2) produces a spanning forest SF ⊂ E
 of the graph G where each connected component contains one local maximum
 of the TO. It is the root of the tree spanning the connected component.
- 2. If we require the TO to form a slope³ T_{max} remains connected and forms a spanning tree of the graph G.
- 3. Independence of edges: All 4-neighbors $(v, w) \in E$ of a spiral TO connect a vertex with even TO(v) and odd TO(w). Then all edges of the subset $SF_0 = \{(v, w) \in SF | TO(v) \text{ is even, } TO(w) \text{ is odd} \}$ are pairwise independent except at branching points of SF i.e., (2,21) and (20,21) in Fig. 6(a). CKs with more than one edge must be contracted sequentially.

Proof. (Independence) Since the boundary of an $m \times n$ image has always an even length 2(m+n-2) the vertex starting the next inner loop of the spiral starts with an odd number (Fig. 6(a)). After contracting all vertices with even rank (except the root) only odd ranks of $TO_0 = TO$ survive. Compacting $TO_{i+1} = (1 + TO_i)/2$ in $G/SF_{i+1}, i = 1, 2, \ldots$ creates again even ranks that can be contracted into their max-link odd neighbors iteratively until the root is left. The compaction of ranks reduces the number of ranks by a factor of two and hence it has logarithmic parallel complexity.

(Spanning forest) Every vertex $v \in V$ creates only one link to its highest neighbor.

³ In a slope region, every pair of vertices is connected by a monotonic path [11].

Since there are no identical ranks in the TO no cycle can be created. Any local extremum cannot link to a neighbor, following the created link backwards determines the receptive field of the extremum that is a connected component.

In Fig. 7 the local maxima are 17 and 18.

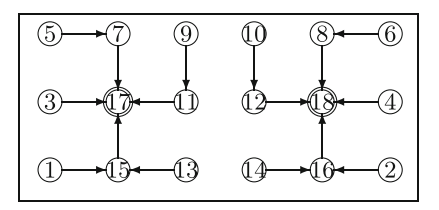


Fig. 7. TO with two local extrema.

(Spanning tree) A slope cannot contain more than one maximum and one minimum [11,13]. Consequently a TO that is a slope has no other extrema than the global extrema and algorithm (2) produces a spanning tree.

5 Combining Contrast Order with TO

The basic strategy is to contract edges with increasing contrast. In real images there are many edges with the same contrast since there are only 256 different contrasts between grey values in the range $0 \le g(v) \le 255$ while image sizes are typically much larger. Hence we aim at using the TO of vertices to deterministically select the edges with same contrast by max-link in the canonical order.

To process several contractions in parallel one further criterion is to group edges that are independent of each other. We observed in Proposition 2 that the spiral TO provides independent subsets of edges by the parity of the ranks of the edge's end points. Special care must be taken (1) at the diagonals from the four corners since CKs contain more than one edge and (2) in the center where the diagonals meet (see Fig. 6(b)). Also there the CKs may be larger. But these cases are limited and do not increase the parallel computational complexity.

5.1 An Upper Bound for the Reconstruction

The reconstruction of the base level of the pyramid can use simple inheritance: lower level vertices just receive the value of their parents from the level above. The graph's structure can be computed from the level above by inverse operations: re-insertion and de-contraction. The base level corresponds to the original structure. Let the values of the original image be $\mathbf{Orig}(v)$, and the values of the reconstruction be $\mathbf{Recon}_t(v)$ with t the top level and $v \in V_0$. Then the quality of reconstruction can be computed as the mean of the pixel-wise absolute difference:

$$MRE_t = \sum_{v \in V} |Orig(v) - Recon_t(v)| / |V_0|$$
(4)

Contracting an edge (v, w) of a contrast c(v, w) = g(v) - g(w), only one of the two vertices v, w survives, $s \in \{v, w\}$. After reconstruction, the end points of the edge will have the same value $g_r(v) = g(s)$ and $g_r(w) = g(s)$ and the difference between the original and the reconstruction will be $|g_r(v) - g(v)| +$

 $|g_r(w) - g(w)| = c(v, w)$. Taking the mean of the absolute differences is directly related to the contrasts:

$$MRE_t(c_t) = \frac{\sum_{(v,w) \in E_c} c(v,w)}{|V_0|} = \frac{\sum_{j=0}^{t-1} c_j \cdot h_0(c_j)}{|V_0|}$$
(5)

In other words we can bound the reconstruction error with the contrast c_t of the highest contracted edge: $\mathbf{MRE}_t(c_t) = \sum_{v \in V} |\mathbf{Orig}(v) - \mathbf{Recon}_t(v)| / |V_0| < c_t$.

5.2 Some Concrete Results

Table 2 lists the maximal number of contractions c_t satisfying $\sum_{c=0}^{c_t} h_0(c) < |V_0|$

for some images from the Berkeley data base [15]. All images have the same size $|V_0| = 154401$, $|V_t|$ is the number of vertices at the top and # crit is the number of critical points (local max, local min, saddle) in the base.

Therefore $MRE_t(c_t)$ of the reconstructed pixel values from the original is 3 and 4 for images Pheasant and Fish, but still below 20 for other images.

Berkelev# Picture $|V_t|$ c_t # crit 43074 4632 Pheasant 3 19788 Fish 210088 9264 18019 9264 41069 squirrel 8 55073 15440 stone statue 12 156065 Coral 13 12352 45915295087 arc 13 12352

19

9264

20541

Table 2. Maximally contractible edges

Empirical tests have shown

(see section Gallery in [9]) that this is below the noticeable deviation for human observers, that can hardly distinguish the reconstruction from the original! A high number of critical points (# crit., i.e., coral) indicates the presence of texture or noise and raises the contrast c_t . To overcome such degradations c_t could be decreased or the brightness contrast could be replaced by a texture contrast.

160068

Cat

6 Conclusion and Outlook

This paper lifts some secrets about the contrast pyramids: the contrast histogram as a tool to determine the maximally possible contrast for contracting edges in the contrast pyramid; the spiral total order together with the max-link strategy determine the ECK for maximally contracting a given image before actually constructing the pyramid. Contrast is calculated from the pixel's brightness but both bottom up reduction as well as top-down refinement use inheritance such that the original color values can be used in the reconstruction. These improvements explain results of reconstructions and allow to adapt the few parameters (like c_t and TO) controlling the pyramid's construction.

There is a wide range of potential applications beyond the efficient derivation of the region adjacency graph in [2]. Using the contrast histogram during reconstruction enables to correctly recompute the values of the non-surviving vertices. For the computation of the max-links also the 8-neighborhood can be used. The inside of a bounding box of an image object can be linearized by a spiral and contrast-contracted as a signature of the object The total order for voxel images in 3D could enable efficient processing of volumetric data like CT or MRI in medical imaging.

Acknowledgement. Great thanks go to Noriane Petit who produced the experimental results with the contrast histogram during her internship in Wien, 2024.

Disclosure of Interests. The author has no competing interest.

References

- Banaeyan, M., Kropatsch, W.G.: Fast labeled spanning tree in binary irregular graph pyramids. J. Eng. Res. Sci. 1(10), 69–78 (2022)
- Banaeyan, M., Kropatsch, W.G., Hladuvka, J.: Redundant 1-cells in multi-labeled 2-Gmap irregular pyramids. In: Bürstmayr, H. et al., (eds.) Proc. OAGM Workshop, Digitalization for Smart Farming and Forestry, pp. 5–22. Technische Universität Graz (2022)
- Batavia, D., Kropatsch, W.G., Casablanca, R.M., Gonzalez-Diaz, R.: Congratulations! Dual graphs are now orientated! In: Conte, D., Ramel, J.-Y., Foggia, P. (eds.) GbRPR 2019. LNCS, vol. 11510, pp. 131–140. Springer, Cham (2019). https://doi.org/10.1007/978-3-030-20081-7 13
- 4. Biggs, N.: Spanning trees of dual graphs. J. Combin. Theory 11, 127–131 (1971)
- Bronstein, M.M., Bruna, J., Cohen, T., Veličković, P.: Geometric deep learning: grids, groups, graphs, geodesics, and gauges. arXiv:2104.13478 (2021)
- Brun, L., Kropatsch, W.G.: Dual contraction of combinatorial maps. In: Kropatsch, W.G., Jolion, J.M. (eds.) 2nd IAPR-TC-15 Workshop on Graph-based Representation, pp. 145–154. OCG-Schriftenreihe, Österreichische Computer Gesellschaft (1999). Band 126
- Brun, L., Kropatsch, W.: Irregular pyramids with combinatorial maps. In: Ferri, F.J., Iñesta, J.M., Amin, A., Pudil, P. (eds.) SSPR /SPR 2000. LNCS, vol. 1876, pp. 256–265. Springer, Heidelberg (2000). https://doi.org/10.1007/3-540-44522-6 27
- 8. Burt, P.J.: A pyramid framework for real-time computer vision. In: Davis, L.S. (ed.) Foundations of Image Understanding, chap. 12, pp. 349–380. Kluwer (2001)
- 9. Cerman, M.: Structurally correct image segmentation using local binary patterns and the combinatorial pyramid. Technical report, PRIP-TR-133, PRIP, TU Wien (2015)
- Cerman, M., et al.: Topology-based image segmentation using LBP pyramids. Mach. Vision Appl. 27(8), 1161–1174 (2016)
- 11. Gonzalez-Diaz, R., Batavia, D., Casablanca, R.M., Kropatsch, W.G.: Characterizing slope regions. J. Combin. Optim. 1–20 (2021)
- Kropatsch, W.G.: Equivalent contraction kernels to build dual irregular pyramids.
 In: Solina, F., Kropatsch, W.G., Klette, R., Bajcsy, R. (eds.) Advances in Computer Science. Advances in Computer Vision, pp. 99–107. Springer, Vienna (1997). https://doi.org/10.1007/978-3-7091-6867-7 11

- 13. Kropatsch, W.G., Banaeyan, M., Gonzalez-Diaz, R.: Controlling topology preserving graph pyramids. In: A.El-Yacoubi, M., Vincent, N., Kurtz, C. (eds.) Emerging Topics in Pattern Rrecognition and Artificial Intelligence, vol. 9, chap. 2, pp. 27–76. World Scientific (2024)
- 14. Mallat, S.G.: A theory for multiresolution signal decomposition: the wavelet representation. IEEE Trans. Pattern Anal. Mach. Intell. **PAMI-11**(7), 674–693 (1989)
- Martin, D.R., et al.: A database of human segmented natural images and its application to evaluating segmentation algorithms and measuring ecological statistics.
 In: 8th International Conference on Computer Vision, ICCV 2001, vol. 2, pp. 416–423 (2001)
- Torres, F., Kropatsch, W.G.: Canonical encoding of the combinatorial pyramid.
 In: Kúkelová, Z., Heller, J. (eds.) Proceedings of the 19th Computer Vision Winter Workshop 2014, pp. 118–125. Křtiny, CZ (2014). iSBN 978-80-260-5641-6